# QSAR and Molecular Shape Analyses of Three Series of 1-(Phenylcarbamoyl)-2-pyrazoline Insecticides

Kathleen A. Rowberg,[†,‡] Mark Even,[†] Eric Martin,[§,∥] and Anton J. Hopfinger*[,†]

Department of Chemistry, M/C 111, University of Illinois at Chicago, Box 6998, Chicago, Illinois 60680, and DowElanco, P.O. Box 68955, Indianapolis, Indiana 46268-1053

Three structurally related series of 1-(phenylcarbamoyl)-2-pyrazolines that exhibit insecticidal activity have been studied in terms of molecular shape and QSAR analyses. The active conformation, in terms of $N^1$-phenylamide and $C^3$-phenyl ring substituents to the pyrazoline ring, could be postulated. The bioactive conformation corresponds to a near all-planar structure. No bioactive conformation could be postulated for phenyl rings on either of the saturated carbons of the pyrazoline ring. However, for $C_4$-phenyl ring substitution, the only stable conformation corresponds to the plane of the phenyl ring being nearly perpendicular to the plane of pyrazoline ring. Dipole moment properties of the substituted phenylamide unit to the $N^1$ of the pyrazoline ring correlate with insecticidal potency. Lipophilicity is not found to be important in dictating insecticidal activity.

## INTRODUCTION

The insecticidal activities within three related analog series of 1-(phenylcarbamoyl)-2-pyrazolines have been reported (Wellinga et al., 1977; van Hess et al., 1978; Grosscurt et al., 1979). The general structures of these three series are given by I–III. Structures I–III also delineate the sites of substituent substitution ($R_x$, $R_y$, and $R_z$) as well as the major torsion angle degrees of freedom ($\theta_1$, $\theta_2$, $\theta_3$, and $\theta_4$) which control the conformational profiles of these molecules.

An inspection of the structure–activity tables of the analogs synthesized and tested for I–III suggested that this dataset might yield promising results from a molecular modeling analysis. There are three primary reasons for making this evaluation. First, a relatively large range of $R_x$, $R_y$, and $R_z$ substituents, in terms of variations in physicochemical properties, were investigated. Next, there was reason to believe that the conformation/molecular shape of the molecule plays a major role in insecticidal activity. Ortho substituents $R_x$ and $R_z$ diminish activity and can alter the conformational profiles of torsion angles $\theta_1$ and $\theta_4$ (Hopfinger and Burke, 1990). Lastly, all compounds were evaluated in a common, and reliable, activity screen.

## METHODS

The lowest compound concentration to realize greater than 90% mortality against *Leptinotarsa decemlineata say* in a semi-*in vivo* medium was used as the measure of relative insecticidal potency. The concentration measures reported in Wellinga et al. (1977), van Hess et al. (1978), and Grosscurt et al. (1979) were used in constructing the quantitative structure–activity relationships (QSARs), but they were expressed as $-\log(C_{90})$, where $C_{90}$ is the lethal concentration in parts per million (ppm).

The molecules were built using standard bond lengths and angles for the phenyl rings. The joint valence geometry of the amide unit and pyrazoline ring proved to be problematic. Of primary concern was the hybridization of the ring nitrogen bonded to the amide carbon. The crystal structure of $N^1$,$N^2$-dibenzoyl-3,5-dimethyl-5-hydrazino-$\Delta^2$-pyrazoline has been reported (Seth and Chaleraborty, 1988). This molecule contains the carbonyl unit bonded to a pyrazole ring at the nitrogen site, and the crystal structure valence geometry of this unit was used as a starting point in a series of quantum mechanical structure optimization studies up to the 6-315* level. The results of these studies will be the subject of another publication (Nicholas et al., 1994). However, the overall results are that the crystal structure geometry is very nearly identical to the geometries optimized in the quantum mechanics calculations. In particular, the ring nitrogen bonded to the amide unit is predominantly $sp^2$ in hybridization. This is in contrast to the situation when a methyl group replaces the amide unit. In this case, the hybridization of the nitrogen is largely $sp^3$. Overall, this suggests that pi-rich systems bonded to the nitrogen promote $sp^2$ character, while saturated substituents induce $sp^3$ valence behavior.

The optimized geometry of the amide–pyrazoline ring moiety, using MNDO (Dewar and Thiel, 1977), was held fixed, as was the valence geometry of the phenyl rings in performing a simultaneous fixed-valence geometry scan (Crawford et al., 1988), about $\theta_1$–$\theta_4$, provided $\theta_2$ was needed. Both the *trans* and *cis* isomers of the amide bond were investigated for some "very active", "average", and "inactive" compounds. The purpose of choosing this subset of compounds from the available SAR tables was to see if the preferred isomer could be identified without having to explore the entire database. The *trans* isomer yielded the lower energy structure (by about 3.5 kcal/mol using MNDO) for all analogs studied and, consequently, was the isomer used in the subsequent conformational searches.

The II and III analogs in the subset of compounds used to study the amide bond isomers were also used to explore the *R*/*S* isomers resulting from the addition of the phenyl ring having the $R_y$ substituents to the pyrazoline ring. No significant differences in conformational energetics were observed between these two isomers for any of the compounds studied. Thus, the *R* isomer was arbitrarily selected in all subsequent structural studies.

The fixed valence geometry conformational scans employed the MM2 nonbonded potentials (Burkert and Allinger, 1982), monopole–monopole electrostatic interactions using a Coulomb potential and CNDO/2 (Pople and Beveridge, 1970), charges with a molecular dielectric of 3.5 (Hopfinger, 1973), the hydrogen bond potential suggested by Hopfinger (1973), and torsional potentials for $\theta_1$–$\theta_4$ derived at the MNDO level of parametrization (Hopfinger and Pearlstein, 1984). The SCAN and INTRADAT options of CHEMLAB-II (1991) were used to identify the apparent conformational energy minima as a function of $\theta_1$–$\theta_4$ at 30° resolution for each torsion angle. Symmetry relationships were used whenever possible to reduce the size of a conformational search. The apparent minima were used as starting points in a

† University of Illinois.
‡ Present address: Department of Chemistry, Addis Ababa University, Box 1176, Addis Ababa, Ethiopia.
§ DowElanco.
∥ Present address: Chiron Corp., 4560 Horton St., Emeryville, CA 94608.

0021-8561/94/1442-0374$04.50/0 © 1994 American Chemical Society

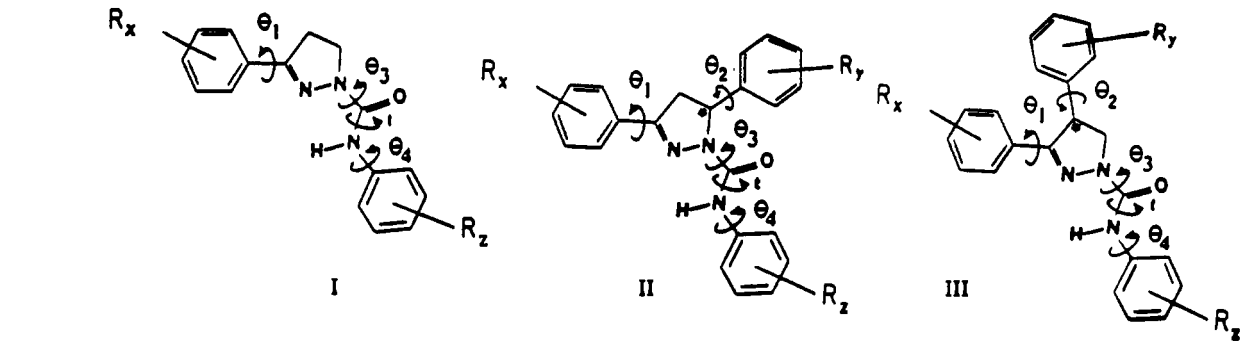


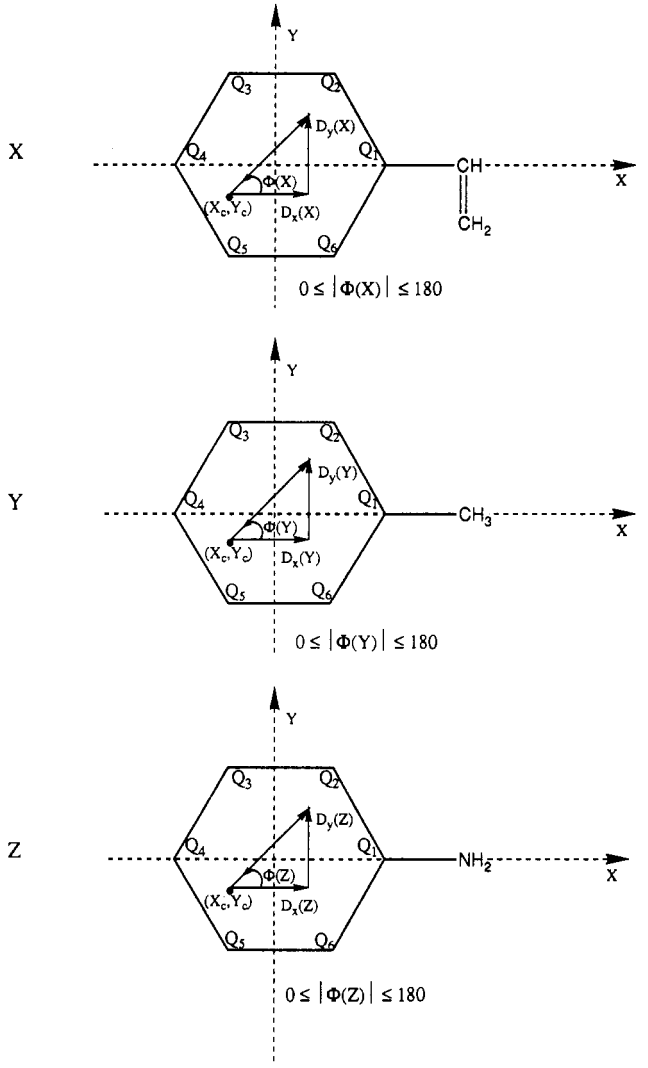


**Figure 1.** Three model compounds used to mimic the electronic properties and, in particular, the dipolar properties of the substituted X, Y, and Z rings. $Q_i$ refer to the residual charges on the ring carbons, and the ($X_c$, $Y_c$) are the coordinates of the center of charge on the model compound.

complete energy minimization as a function of the torsion angles $\Theta_1$–$\Theta_4$ using the CHEMLAB-II (1991) minimizer.

The individual dipole moment properties of the phenyl rings denoted $X(R_x)$, $Y(R_y)$, and $Z(R_z)$ were computed using the model compounds shown in Figure 1. The respective groups attached at the $C_1$ atoms were chosen to mimic the local structural environment of each ring when part of the complete (phenylcarbamoyl)pyrazoline. The charges and dipole properties were taken from CNDO/2 calculations on the model compounds. $D_x$ is the dipole component in the direction of the bond joining the phenyl and pyrazoline rings. $D_y$ is the in-plane perpendicular dipole component to $D_x$, ($X_c$, $Y_c$) denotes the location of the center of charge in the ring plane, and $\Phi$ is the angle the total dipole makes with $D_x$. The partial atomic charges are denoted by $Q_i$. The substituent water/octanol partition coefficients, the $\Pi$ constants, $\Pi(R_\alpha)$, where $\alpha$ = x,y,z of the rings, were taken from the values reported by Hansch and Leo (1979).

Molecular shape analysis (MSA) (Hopfinger and Burke, 1990) was used to construct molecular shape descriptors for QSAR studies. The class I analog having $R_x = R_z$ = 4-Cl (compound 12 of Table 1), in the postulated active conformation (see Results), was used as the shape reference compound. Each intramolecular minimum energy conformation within 5 kcal/mol of the global minimum of each analog in the SAR tables was superimposed on the shape reference compound. The criterium for molecular superposition was to place the pyrazoline rings of the shape reference and the comparison analog in common. The common overlap steric volume (COSV) of the shape reference and comparison analog was used as a scalar measure of molecular shape similarity (Hopfinger and Burke, 1990). The COSV jointly takes into account molecular flexibility and structural diversity in comparing molecular shapes. In addition, the absolute differences in the $\Theta_1$ and $\Theta_4$ torsion angle rotations, $|\Delta\Theta_1|$ and $|\Delta\Theta_4|$, respectively, for the shape reference and comparison analogs were also used as relative measures of molecular shape similarity. The absolute torsion angle differences are direct measures of local changes in molecular shape as a function of molecular flexibility.

## RESULTS

The 35 class I analogs used in the MSA–QSAR analysis are reported in Table 1 along with their corresponding $-\log(C_{90})$ insecticidal activity measures. Table 1 also contains the physicochemical descriptors that were determined to yield the most significant MSA–QSAR. The following section discusses how the MSA–QSAR for the class I analogs was constructed.

**1. Log *P* and $\Pi(R_\alpha)$.** It was relatively straightforward to demonstrate that the estimated relative lipophilicity of $R_x$, $R_y$, or $R_z$ and total lipophilicity, log *P*, have virtually no influence on insecticidal potency. Figure 2a is a plot of $-\log(C_{90})$ vs $\Pi(R_x)$ for three class I analogs. The $-\log(C_{90})$ increases by about 2 log units as $R_x$ goes from 2-Cl to 3-Cl and to 4-Cl with $R_z$ held at 4-Cl. Overall, the net log *P* values of these three compounds are essentially equal to one another.

Figure 2b is an equivalent plot to Figure 2a but for $\Pi(R_z)$ vs $-\log(C_{90})$ for $R_x = R_y$ = 4-Cl for three class III compounds. Just as for $R_x$, it is observed in Figure 2b that $-\log(C_{90})$ increases, about 3 log units in this example, as the series goes from $R_z$ = 2-Cl to 3-Cl to 4-Cl. Once again, the log *P* values of the three analogs are about equal.

Figure 2c is a plot of $\Pi(R_z)$ vs $-\log(C_{90})$ for $R_x = R_y$ = 4-Cl for some para-substituted $R_z$ class III analogs. No correlation between para substituent $\Pi$ values and $-\log(C_{90})$ is evident in this plot. Total lipophilicity ($\Pi(R_x) + \Pi(R_y) + \Pi(R_z)$) for para substituent analogs only in class III is plotted against $-\log(C_{90})$ in Figure 2d. There appears to be a trend in which $-\log(C_{90})$ increases with an increase in ($\Pi(R_x) + \Pi(R_y) + \Pi(R_z)$). However, the least and most active analogs have the same total lipophilicity.

The addition of the Y ring, at least for the class III analogs, enhances activity as compared to equivalent class I analogs. This is shown in Figure 2e, where ($\Pi(R_x)$ +

Table 1. 35 Class I Analogs and Corresponding $-\log(C_{90})$ Measures Used To Construct Eqs 1 and 2[a]

| no. | $R_x$ | $R_z$ | obsd $-\log(C_{90})$ | pred $-\log(C_{90})$ | residual | $D_T(X)$, D | $\Phi(X)$, deg | $D_x(Z)$, D | $\Phi(Z)$, deg | $\Delta\Theta_1$, deg | $\Delta\Theta_4$, deg | $I_5$ |
|---|---|---|---|---|---|---|---|---|---|---|---|---|
| 1 | H | H | 4.00 | 4.08 | −0.08 | 0.20 | 0 | 1.4 | 0 | 1.0 | 13.0 | 0 |
| 2 | H | 4-F | 4.52 | 4.53 | −0.01 | 0.20 | 0 | 3.0 | 0 | 1.2 | 12.2 | 0 |
| 3 | H | 4-Cl | 5.52 | 4.90 | 0.62 | 0.20 | 0 | 3.8 | 0 | 1.4 | 7.5 | 0 |
| 4 | H | 3,4-$Cl_2$ | 5.00 | 4.88 | 0.12 | 0.20 | 0 | 4.6 | 32 | 3.6 | 9.2 | 0 |
| 5 | 4-Cl | H | 4.52 | 4.17 | 0.35 | 2.59 | 0 | 1.4 | 0 | 1.5 | 11.2 | 0 |
| 6 | 4-Cl | 2-$CH_3$ | 3.52*[b] | 3.51 | 0.01 | 2.59 | 0 | 1.4 | 0 | 1.3 | 23.9 | 0 |
| 7 | 4-Cl | 4-$CH_3$ | 4.52 | 4.35 | 0.17 | 2.59 | 0 | 1.3 | 0 | 0.7 | 7.5 | 0 |
| 8 | 4-Cl | 4-F | 5.00 | 4.80 | 0.20 | 2.59 | 0 | 3.0 | 0 | 1.0 | 7.0 | 0 |
| 9 | 4-Cl | 2-Cl | 3.22* | 3.33 | −0.11 | 2.59 | 0 | 0.4 | 89 | 1.0 | 21.0 | 0 |
| 10 | 4-Cl | 3,4-$Cl_2$ | 5.00 | 4.86 | 0.14 | 2.59 | 0 | 4.6 | 32 | 1.2 | 10.1 | 0 |
| 11 | 4-Cl | 3-Cl | 4.00 | 4.30 | −0.30 | 2.59 | 0 | 2.5 | 50 | 0.5 | 14.6 | 0 |
| 12 | 4-Cl | 4-Cl | 5.52 | 4.84 | 0.68 | 2.59 | 0 | 3.8 | 0 | 0.3 | 9.0 | 0 |
| 13 | 4-Cl | 3-$NO_2$ | 4.00 | 4.91 | −0.91 | 2.59 | 0 | 4.1 | 48 | 0.9 | 8.3 | 0 |
| 14 | 4-Cl | 4-$NO_2$ | 5.00 | 4.97 | 0.03 | 2.59 | 0 | 7.2 | 0 | 1.0 | 8.0 | 0 |
| 15 | 4-Cl | 4-CN | 5.52 | 5.02 | 0.50 | 2.59 | 0 | 5.0 | 0 | 0.7 | 7.8 | 0 |
| 16 | 4-Cl | 3-$CF_3$ | 5.00 | 4.74 | 0.26 | 2.59 | 0 | 3.2 | 41 | 0.5 | 9.0 | 0 |
| 17 | 4-Cl | 4-$CF_3$ | 6.00 | 4.99 | 1.01 | 2.59 | 0 | 5.1 | 0 | 0.6 | 8.5 | 0 |
| 18 | 3-Cl | 4-Cl | 4.52 | 4.81 | −0.29 | 3.30 | 66 | 3.8 | 0 | 2.5 | 9.1 | 0 |
| 19 | 3-Cl | 3,4-$Cl_2$ | 4.00 | 4.83 | −0.83 | 3.30 | 66 | 4.6 | 32 | 3.0 | 10.3 | 0 |
| 20 | 3,4-$Cl_2$ | 4-Cl | 5.00 | 4.82 | 0.18 | 4.54 | 41 | 3.8 | 0 | 2.4 | 8.8 | 0 |
| 21 | 3,5-$Cl_2$ | 4-Cl | 3.52 | 3.51 | 0.01 | 2.42 | 0 | 3.8 | 0 | 3.0 | 8.1 | 1 |
| 22 | 2-Cl | 4-Cl | 4.00 | 3.69 | 0.31 | 3.18 | 86 | 3.8 | 0 | 86.0 | 8.6 | 0 |
| 23 | 2,4-$Cl_2$ | 4-$CH_3$ | 2.78* | 3.22 | −0.44 | 3.37 | 64 | 1.3 | 0 | 84.2 | 7.3 | 0 |
| 24 | 3-$NO_2$ | 4-Cl | 4.52 | 4.88 | −0.36 | 5.87 | 57 | 3.8 | 0 | 2.6 | 7.6 | 0 |
| 25 | 3-$NO_2$ | 3,4-$Cl_2$ | 3.52 | 4.85 | −1.33 | 5.87 | 57 | 4.6 | 32 | 2.1 | 10.0 | 0 |
| 26 | 4-F | 4-Cl | 5.52 | 4.92 | 0.60 | 1.85 | 0 | 3.8 | 0 | 1.0 | 7.3 | 0 |
| 27 | 4-F | 3,4-$Cl_2$ | 4.52 | 4.97 | 0.45 | 1.85 | 0 | 4.6 | 32 | 1.1 | 8.1 | 0 |
| 28 | 4-$CH_3$ | 4-$CH_3$ | 4.52 | 4.31 | 0.21 | 0.01 | 0 | 1.2 | 0 | 0.8 | 7.5 | 0 |
| 29 | 4-$CH_3$ | 4-Cl | 4.52 | 4.91 | −0.39 | 0.01 | 0 | 3.8 | 0 | 0.7 | 7.6 | 0 |
| 30 | 4-Cl | 3,5-$Cl_2$ | 3.22* | 3.49 | −0.27 | 2.59 | 0 | 3.5 | 0 | 0.8 | 8.1 | 1 |
| 31 | 4-Cl | 2,4-$Cl_2$ | 4.00 | 4.06 | −0.06 | 2.59 | 0 | 2.8 | 50 | 1.0 | 20.3 | 0 |
| 32 | 4-Cl | 2,5-$Cl_2$ | 2.20* | 2.32 | −0.12 | 2.59 | 0 | 1.5 | 15 | 0.9 | 21.6 | 1 |
| 33 | 4-Cl | 2,4,5-$Cl_3$ | 3.22* | 2.68 | 0.54 | 2.59 | 0 | 3.6 | 6 | 0.8 | 23.9 | 1 |
| 34 | 4-Cl | 3,4,5-$Cl_3$ | 3.52* | 3.68 | −0.16 | 2.59 | 0 | 5.4 | 0 | 1.2 | 7.9 | 1 |
| 35 | 2-Cl | 3,4-$Cl_2$ | 4.00 | 3.82 | 0.18 | 3.18 | 86 | 4.6 | 32 | 85.1 | 8.1 | 0 |

[a] The QSAR descriptors and predicted and residual activities, using eq 1, are also given. [b] Asterisks indicate compounds having activities ≤3.52; the values given were estimated from linear interpolation of the original activity plots.

$\Pi(R_z)$) for ortho substituent analogs common to classes I and III are plotted against $-\log(C_{90})$. The "intrinsic" increase in $-\log(C_{90})$ for the addition of the Y ring is not constant but depends upon $R_x$ and $R_z$.

Conformational scans about torsional angles $\Theta_1$, $\Theta_3$, and $\Theta_4$ were carried out for the four class I compounds reported in Table 2A. Compound 1 ($R_x = R_y = H$) was chosen as a "standard" in that it should be the most flexible analog in the series since it has no substituents to introduce steric constraints. The other three compounds in Table 2A were selected because their log $P$ values could be about the same, and, therefore, the differences in their observed activities should be due to conformational-dependent properties. Compound 12 ($R_x = R_z$ = 4-Cl) has a conformational profile virtually identical to that of compound 1 as can be seen from their conformational energy maps in Figures 3 (compound 1) and 4 (compound 12). Rigorous energy minimizations yield 4-fold degenerate global minima at the torsion angle values reported in Table 2A. These four conformations essentially correspond to an all-planar conformation which is shown in Figure 5 for compound 12.

Compounds 9 and 22 each have distinctly different conformational profiles from one another and from compounds 1 and 12, as can be seen in their conformational energy maps shown in Figures 6 (compound 9) and 7 (compound 22). In particular, these relatively inactive analogs cannot energetically adopt the near all-planar conformation found to be, essentially, the global minimum energy conformation for compound 1 and also for the very active analog, compound 12. Hence, we postulate that the all-planar conformation, shown in Figure 5 for compound 12, is close to the bioactive conformation for the series I analogs.

The difference in activities of compounds 1 and 12 cannot be explained on the basis of the postulated bioactive conformation. Hence, other physicochemical properties were investigated to account for the unresolved differences in activities not accounted for by conformational behavior. It was found that the $x$-component of the Z-ring dipole, $D_x(Z)$ ($x$ is the direction of the C–N (pyrazoline) bond) for the model compound in Figure 1 correlates with activity. This dipole measure is independent of the remainder of the whole molecule. Also, the absolute values of the angles between the $x$-axis and the total dipole moments of the X- and Z-ring model compounds (Figure 1), $|\Phi(X)|$ and $|\Phi(Z)|$, respectively, correlate with activity. The corresponding QSAR is

$$-\log(C_{90}) = 0.698D_x(Z) - 0.062D_x(Z)^2 - 0.014|\Phi(X)| - 0.012|\Phi(Z)| - 1.842I_5 + 3.43 \quad (1)$$

$$N = 35,\ R = 0.905,\ S = 0.40,\ F = 25.3D_x(Z)_{opt} = 5.6\ D$$

$I_5$ in eq 1 is an indicator variable to indicate the presence of a 5-position substituent ($I_5 = 1$) or the absence ($I_5 = 0$) of this substituent on either the X or Z ring. The values of the QSAR descriptors for the 35 analogs are given as part of Table 1 along with the predicted activities and residuals using eq 1. $D_x(Z)_{opt}$ refers to the value of the $x$-component of the Z-ring dipole which maximizes $-\log(C_{90})$ in eq 1.

An attempt was also made to include the propensity of an analog to adopt the postulated bioactive conformation

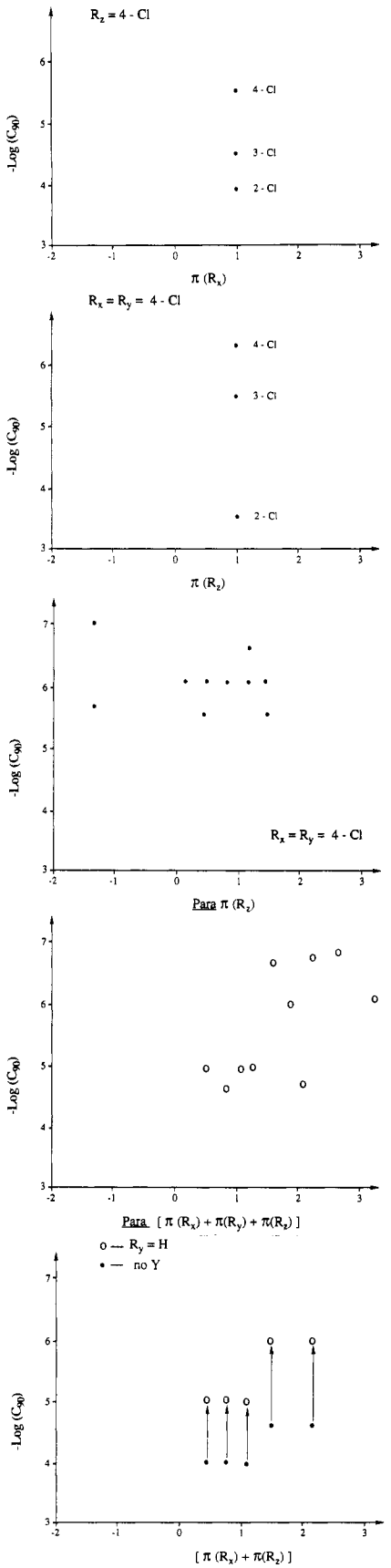


**Figure 2.** (a–e, top to bottom) (a) Example of constant $\Pi(R_x)$ (lipophilicity) of $R_x$ on observed insecticidal potency for a fixed lipophilicity, $R_z$ = 4-Cl, in three class I analogs. (b) Same as (a) but for $\Pi(R_z)$ vs $-\log(C_{90})$ with $R_x = R_y$ = 4-Cl. (c) Same as (a) but for $\Pi(R_z)$ for para substituents vs $-\log(C_{90})$ with $R_x = R_y$ = 4-Cl. (d) Same as (a) but for the sum of the lipophilicities of para substituents ($\Pi(R_x) + \Pi(R_y) + (R_z)$) vs $-\log(C_{90})$. Same as (a) but for ($\Pi(R_x) + \Pi(R_z)$) vs $-\log(C_{90})$ for compounds with $R_y$ = H (class III) (open circles) and corresponding class I analogs (solid circles).

**Table 2. Class I–III Analogs Used in the Conformational Analyses[a]**

A. Class I Analogs

| no. | $R_x$ | $R_z$ | $-\log(C_{90})$ | $\Theta_1$, deg | $\Theta_3$, deg | $\Theta_4$, deg |
|---|---|---|---|---|---|---|
| 1 | H | H | 4.00 | 0 | ±19 | ±11 |
| 9 | 4-Cl | 2-Cl | 3.22 | ±3 | ±22 | −123 |
| 12 | 4-Cl | 4-Cl | 5.52 | 0 | ±21 | ±9 |
| 22 | 2-Cl | 4-Cl | 4.00 | 86 | ±22 | ±13 |

B. Class II Analogs

| no. | $R_x$ | $R_y$ | $R_z$ | $-\log(C_{90})$ | $\Theta_1$, deg | $\Theta_3$, deg | $\Theta_4$, deg |
|---|---|---|---|---|---|---|---|
| 36 | 4-Cl | 4-Cl | 4-Cl | 5.52 | 0 | ±13 | ±9 |
| 37 | 4-Cl | 2-Cl | 4-Cl | 4.52 | 0 | ±16 | ±9 |

C. Class III Analogs

| no. | $R_x$ | $R_y$ | $R_z$ | $-\log(C_{90})$ | $\Theta_1$, deg | $\Theta_3$, deg | $\Theta_4$, deg |
|---|---|---|---|---|---|---|---|
| 54 | 4-Cl | 4-Cl | 4-Cl | 6.52 | ±4 | ±20 | ±9 |

[a] The values of the Θ torsion angles corresponding to global minimum energy conformations are given.

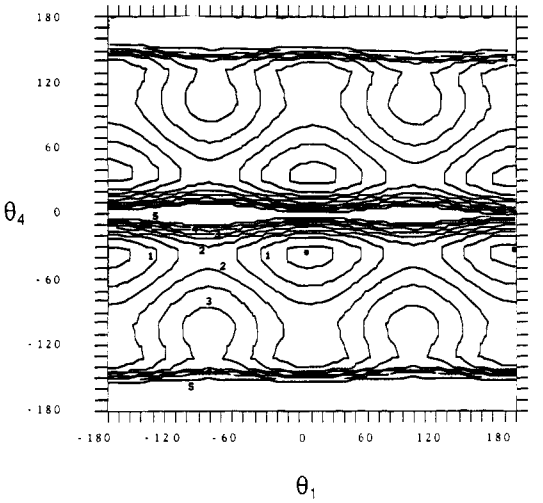


**Figure 3.** Conformational energy map of ($\Theta_1$, $\Theta_4$) vs energy for compound 1. The energy contours are in kilocalories per mole above the global minimum, denoted by ●. $\Theta_1 = \Theta_4 = 0°$ denotes the planar conformation shown for I. $\Theta_3$ was fixed at 30° from planar.

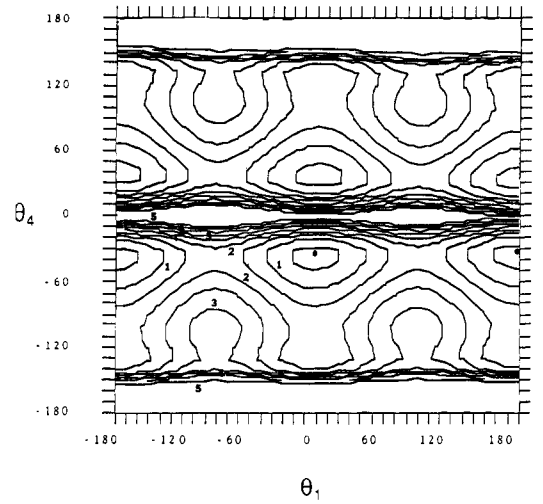


**Figure 4.** Same as Figure 3 but for compound 12.

in a QSAR. The most significant QSAR found is

$$-\log(C_{90}) = 0.402D_x(Z) - 0.034D_x^2(Z) - 0.014|\Theta(X)| - 0.052|\Theta(Z)| - 1.344I_5 + 4.28 \quad (2)$$

$$N = 35,\ R = 0.841,\ S = 0.51,\ F = 13.8D_x(Z)_{opt} = 5.9\ D$$

$D_x(Z)$ and $I_5$ are the same as in eq 1, and $|\Delta\Theta_i|$ refers to the absolute difference in torsion angle $\Theta_i$ in the global

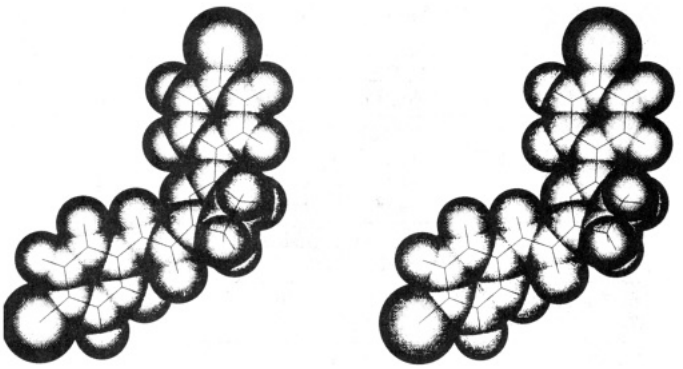

**Figure 5.** Stereo representation of compound **12** in the all-planar conformation.

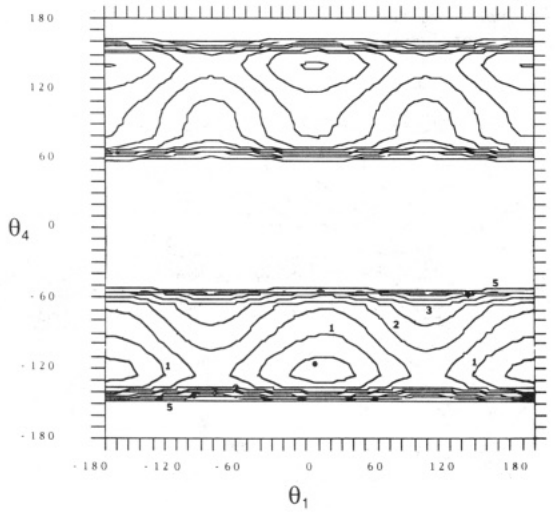


**Figure 6.** Same as Figure 3 but for compound **9**.

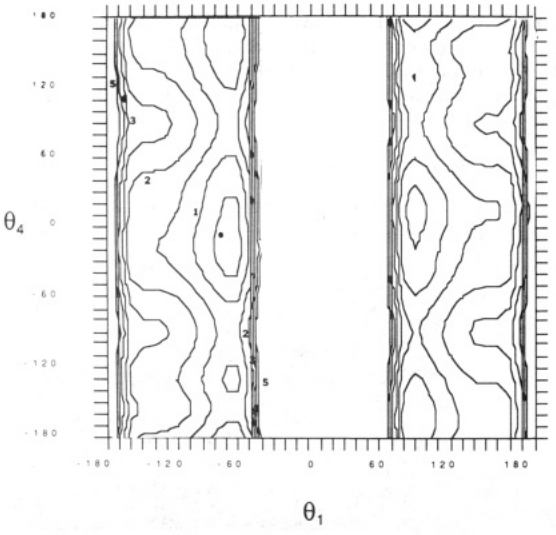


**Figure 7.** Same as Figure 3 but for compound **22**.

minimum energy conformation from the near all-planar (bioactive) conformation. Clearly, eq 2 is inferior to eq 1 as reflected in $R$, $S$, and $F$. However, the dependence of both QSARs on $D_x(Z)$ and $I_5$ suggests these two descriptors are key to explaining the variations in $-\log(C_{90})$ in series I analogs. Moreover, the optimum values of $D_x(Z)$ in both QSARs are virtually the same, which suggests a reliable and stringent structural constraint to optimize activity.

The conformational analyses of the series II and III analogs were carried out with $\Theta_1$, $\Theta_3$, and $\Theta_4$ locked into the bioactive torsion angle states postulated for the series I analogs. The idea behind imposing this conformational constraint is that some of the series I compounds are quite

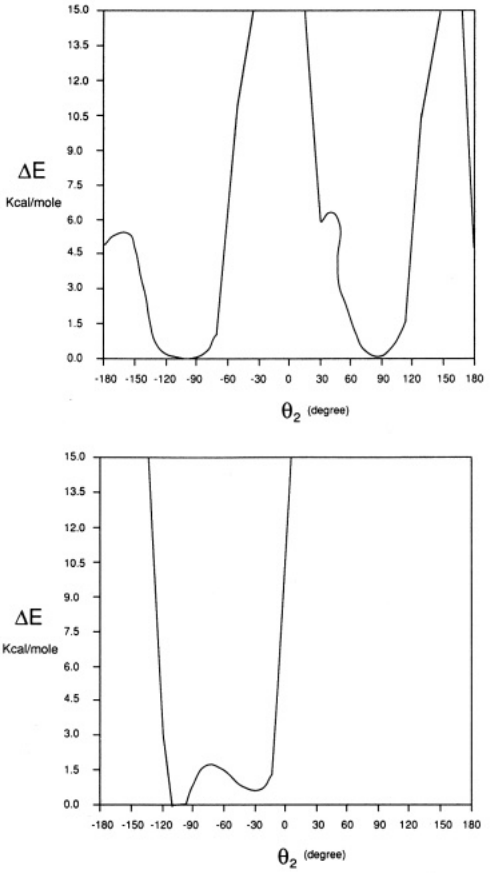


**Figure 8.** Conformational energy plots for $\Theta_2$ of the $R$ isomers of two class II analogs. The other torsion angles were fixed at $\Theta_1 = 0°$, $\Theta_3 = 30°$, and $\Theta_4 = -9°$: (a) compound **36**, $R$ isomer; (b) compound **37**, $R$ isomer.

active relative to series II and III compounds. Hence, the class II and III compounds must adopt the bioactive conformation of the series I analogs as a necessary condition to be active insecticides. The Y ring introduces two possible isomer states for each class II and class III analog. Conformational scans were carried out for torsion angle $\Theta_2$ for both possible isomers for both class II and III analogs.

Two class II analogs having $R_x = R_z$ = 4-Cl, which are identical to compound **12** with regard to X- and Z-ring substituents, were studied. The conformational energy plots of one of the two isomers for $\Theta_2$ are given in Figure 8 for the two analogs. The $\Theta_2 = 0°$ conformation corresponds to the plane of the phenyl ring being perpendicular to the pyrazoline ring and bisecting the N–C*–C bond angle. The two isomers of each analog have nearly identical conformational profiles reflecting the near planarity of the pyrazoline ring. Conversely, the conformational profiles of the two analogs are quite different from one another. Compound **37**, which is 10-fold less active than compound **36**, cannot adopt the minimum energy state available to **36** at $\Theta_2 = 85°$. This conformation corresponds to the 2-Cl of compound **37** having a forbidden steric interaction with the carbonyl oxygen. However, $\Theta_2 = 85°$ cannot be postulated to be the bioactive conformation since, by symmetry, the other energy minimum at $\Theta_2 = -95°$ is identical to $\Theta_2 = 85°$ for compound **36**. The loss in activity of compound **37**, relative to **36**, might better be explained by an intermolecular interaction of the carbonyl oxygen with a site on the receptor. The 2-Cl of compound **37** may interfere with this interaction. There is no basis to postulate the "active isomer" from these conformational analyses.

The reported substituent variation in the class II analogs (van Hess et al., 1978) is not sufficient to permit a reliable

Table 3. 25 Class III Analogs and Corresponding $-\log(C_{90})$ Measures Used To Construct Eq 3[a]

| no. | $R_x$ | $R_y$ | $R_z$ | obsd $-\log(C_{90})$ | pred $-\log(C_{90})$ | residual | $D_x(Z)$, D | $D_x(Y)$, D | $D_x(X)$, D | $\Phi(Z)$, deg |
|---|---|---|---|---|---|---|---|---|---|---|
| 38 | H | H | H | 5.00 | 5.00 | 0.00 | 1.4 | 0.2 | 0.2 | 0 |
| 39 | H | H | 4-Cl | 6.52 | 6.45 | 0.07 | 3.9 | 0.2 | 0.2 | 0 |
| 40 | H | H | 4-$NO_2$ | 6.00 | 6.04 | −0.04 | 7.2 | 0.2 | 0.2 | 0 |
| 41 | H | 4-Cl | H | 5.00 | 5.00 | −0.00 | 1.4 | 2.6 | 0.2 | 0 |
| 42 | H | 4-Cl | H | 5.00 | 5.00 | −0.00 | 1.4 | 2.6 | 0.2 | 0 |
| 43 | H | 4-Cl | 3,4-$Cl_2$ | 6.52 | 6.30 | 0.22 | 4.6 | 2.6 | 0.2 | 32 |
| 44 | 4-Fl | H | H | 4.52 | 5.00 | −0.48 | 1.4 | 0.2 | 1.9 | 0 |
| 45 | 4-Fl | H | 4-Cl | 6.00 | 6.45 | −0.45 | 3.9 | 0.2 | 1.9 | 0 |
| 46 | 4-Cl | H | H | 5.00 | 5.00 | 0.00 | 1.4 | 0.2 | 2.6 | 0 |
| 47 | 4-Cl | H | 2-Cl | 3.22 | 3.21 | 0.01 | 0.4 | 0.2 | 2.6 | 89 |
| 48 | 4-Cl | H | 4-Cl | 6.52 | 6.45 | 0.07 | 3.9 | 0.2 | 2.6 | 0 |
| 49 | 4-Cl | H | 4-CN | 6.00 | 6.60 | −0.61 | 5.0 | 0.2 | 2.6 | 0 |
| 50 | 4-Cl | 4-Cl | H | 5.52 | 5.00 | 0.52 | 1.4 | 2.6 | 2.6 | 0 |
| 51 | 4-Cl | 4-Cl | 4-F | 6.00 | 6.10 | −0.10 | 3.0 | 2.6 | 2.6 | 0 |
| 52 | 4-Cl | 4-Cl | 2-Cl | 3.22 | 3.21 | 0.01 | 0.4 | 2.6 | 2.6 | 89 |
| 53 | 4-Cl | 4-Cl | 3-Cl | 5.52 | 5.38 | 0.14 | 2.5 | 2.6 | 2.6 | 50 |
| 54 | 4-Cl | 4-Cl | 4-Cl | 6.52 | 6.44 | 0.07 | 3.9 | 2.6 | 2.6 | 0 |
| 55 | 4-Cl | 4-Cl | 4-$CF_3$ | 7.00 | 6.60 | 0.40 | 5.0 | 2.6 | 2.6 | 0 |
| 56 | 4-Cl | H | 3-$CF_3$ | 5.52 | 5.83 | −0.31 | 3.2 | 0.2 | 2.6 | 41 |
| 57 | 4-Cl | H | 4-$CF_3$ | 7.00 | 6.60 | 0.40 | 5.0 | 0.2 | 2.6 | 0 |
| 58 | 4-Cl | 4-Cl | 3-$NO_2$ | 6.00 | 6.07 | −0.07 | 4.1 | 2.6 | 2.6 | 48 |
| 59 | 4-Cl | 4-Cl | 4-$NO_2$ | 6.00 | 6.04 | −0.04 | 7.2 | 2.6 | 2.6 | 0 |
| 60 | 4-Cl | 4-$NO_2$ | H | 5.00 | 5.00 | 0.00 | 1.4 | 6.7 | 2.6 | 0 |
| 61 | 4-Cl | 4-$NO_2$ | 4-Cl | 6.00 | 6.45 | −0.45 | 3.9 | 6.7 | 2.6 | 0 |
| 62 | 4-$CH_3$ | 4-Cl | 4-Cl | 7.00 | 6.45 | 0.55 | 3.9 | 2.6 | 0.9 | 0 |

[a] The QSAR descriptors and predicted and residual activities are also given.

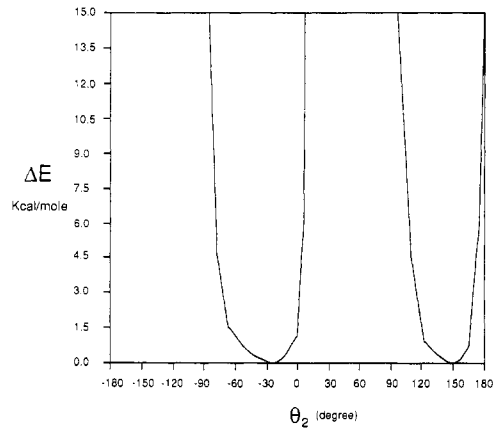


**Figure 9.** Conformational energy plot for $\Theta_2$ of the *R* isomer of a class III analog, compound **54**. The other torsion angles were fixed at $\Theta_1 = 4°$, $\Theta_3 = 21°$, and $\Theta_4 = -9°$.

QSAR analysis. Hence, there are no QSARs similar to eqs 1 and 2 reported for class II analogs.

A set of 25 class III analogs, reported in Table 3, were available for both conformational and QSAR analyses. Unfortunately, there is either no Y-ring substituent, or only a para-Y-ring substituent, for this set of analogs. Consequently, it is not possible to explore any conformation–activity relationship involving $\Theta_2$. Compound **54** of Table 2C, which is the equivalent of compound **36** in the class II series, was studied in terms of its $\Theta_2$ conformational profile. The conformational analysis was performed in the same manner as described for the class II analogs. Both isomers were considered and give virtually identical conformational profiles, again reflecting the near planarity of the pyrazoline ring. The $\Theta_2$ energy plot of the *R* isomer of compound **54** is shown in Figure 9. The minimum energy $\Theta_2$ conformer states have the phenyl ring nearly perpendicular to the pyrazoline ring. Presumably, one of the two equivalent minimum energy conformations of compound **54**, due to the symmetric 4-Cl with respect to $\Theta_2$, is the bioactive conformer.

The class III series can be viewed as structural analogs to the class I series of compounds. Hence, we thought it reasonable that a QSAR for the class III series "incorporate" the features of the class I QSARs. The descriptors used in eqs 1 and 2 were used in combination with dipole, lipophilic, and conformational (value of $\Theta_2$ and common overlap volume (Hopfinger and Burke, 1990) properties of the Y ring in the QSAR analysis. The optimum equation that could be developed is

$$-\log(C_{90}) = 1.220D_x(Z) - 0.121D_x(Z)^2 - 0.009|\Phi(Z)| + 3.53 \quad (3)$$

$$N = 25,\ R = 0.957,\ S = 0.32,\ F = 76.0D_x(Z)_{opt} = 5.0\ D$$

The descriptors in eq 3 are the same as in eq 1. Equation 3 suggests that the variance in insecticidal potency is explained by the dipolar properties of the substituted Z ring. The lack of substituent diversity at rings X and Y for the analogs in Table 3 used to construct eq 3 dilute the physicochemical contributions of these rings to the overall SAR behavior. Consequently, the X- and Y-ring structure–activity information is filtered out of the regression fitting procedure. However, $R_x$ and $R_y$ do have some control over the insecticidal potency, as can be seen by comparing the activities of compounds in Table 3 which, for example, have a common $R_z$ = 4-Cl substituent.

Finally, eq 3 indicates that the optimum value of $D_x(Z)$ is 5.0 D to maximize insecticidal potency. This $D_x(Z)_{opt}$ value is slightly smaller than found for eqs 1 and 2. In composite, the three QSARs developed in this study suggest that $D_x(Z)$ is a key feature for activity.

## DISCUSSION

The postulated bioactive conformation for the class I analogs corresponds to a near-planar geometry of the entire molecule with the carbonyl oxygen of the amide unit *trans* to the double-bond nitrogen of the pyrazoline ring. Planarity of the pyrazoline ring is due to the $sp^2$ character of nitrogen bonded to the amide unit. The $sp^2$ character of the nitrogen is induced by resonance interactions with the amide unit according to molecular orbital calculations, which is also consistent with crystal structure data (Dan and Chakraborty, 1988). Significant excursions from molecular planarity can occur in the torsion angles, especially $\Theta_1$, without major expenditures in conformational energy. Thus, postulating a near planar confor-

mation as the bioactive conformation should be viewed as only an approximate model.

It is not possible to meaningfully postulate the Y-ring bioactive conformation or the bioactive Y-ring isomer of the class II and III analogs. The postulated bioactive conformer state of class I analogs is assumed for class II and III analogs. Under this constraint the only conformations available to the Y ring for class III analogs corresponds to the plane of the phenyl ring being nearly perpendicular to the remainder of the molecule. In the case of class II analogs it appears that the Y-ring substituents that are near the carbonyl oxygen for low-energy Y-ring conformer states interfere with an intermolecular binding interaction and, consequently, lower potency.

Lipophilicity does not appear to govern insecticidal potency. Electronic properties of the entire molecule, such as the dipole moment of the molecule, also do not appear to be related to insecticidal potency. However, *individual* dipolar properties of X and Z rings strongly relate to observed potency and can be used to construct QSARs. In particular, the magnitude of the dipole component of the Z ring parallel to the direction of the bond joining the ring to the amide group is strongly correlated to bioactivity having a value of about 5.5 D to maximize insecticidal potency. The structure–activity data for class II and III analogs is too limited to permit a QSAR evaluation of the Y-ring dipole–insecticidal potency relationship.

An indicator variable, $I_5$, indicating the presence/absence of a 5-position substituent on either the X or Z ring, was needed to account for the low activity of these analogs in the class I series QSARs. The interpretation of $I_5$ is that the receptor pocket cannot accommodate analogs having the bulk of a 5-position substituent on either the X or Z ring.

Overall, the findings from this study may permit the possible generation of new lead insecticide candidates by using the postulated bioactive conformation (molecular shape) as a design template. That is, the postulated bioactive conformation of compound 17 ($R_x$ = 4-Cl, $R_y$ = 4-$CF_3$, $-\log(C_{90})$ = 6.00), for example, may provide a set of constraints to construct a structure which is not based upon a pyrazoline–amide nucleus but has molecular shape and electronic features equivalent to those of compound 17 to confer insecticidal activity. The QSARs reported in this paper should permit a credible prediction of the insecticidal activity in the class I analogs in advance of synthesis. This predictive capability should, in turn, facilitate lead optimization in class I analogs. Similar lead optimization might be possible for class II and III analogs, although certain key analogs in each of these two series should be made and tested to enhance the reliability of the corresponding QSARs.

ACKNOWLEDGMENT

We very much appreciate the financial support of DowElanco. The resources of the Laboratory of Molecular Design at UIC were used to perform this study. We acknowledge the many useful discussions and comments of D. Camper, D. Pernich, C. Manly, K. McLaren, J. Pechacek, M. Ricks, Y. Tong, and G. Bradfisch, all of DowElanco at the time this study was performed.

LITERATURE CITED

Burkert, U.; Allinger, N. L. *Molecular Mechanics*; ACS Monograph 177; American Chemical Society: Washington, DC, 1982.

CHEMLAB-II V 12.0, Molecular Simulations, Inc., Burlington, MA, 1991.

Crawford, R. J.; Pearlstein, R. A.; Mabilia, M.; Hopfinger, A. J. Characterization and Selection of Atom-Pair Potential Functions for Conformational Analysis. *Tetrahedron Comput. Methodol.* **1988**, *1*, 185–206.

Dan, J.; Seth, S.; Chakraborty, S. The Crystal Structure of N′,N²′-Dibenzoyl-3-5-Dimethyl-5-Hydrazino-$\Delta^2$-Pyrazolines. *Indian J. Phys. Chem.* **1988**, *62A*, 455–462.

Dewar, M. J. S.; Thiel, W. Ground States of Molecules, 38. The MNDO Method, Approximations and Parameters. *J. Am. Chem. Soc.* **1977**, *99*, 4899–4906.

Grosscurt, A. C.; van Hes, R.; Wellinga, K. 1-Phenylcarbamoyl-2-pyrazolines: A New Class of Insecticides. 3. Synthesis and Insecticidal Properties of 3,4-Diphenyl-1-phenylcarbamoyl-2-pyrazolines. *J. Agric. Food Chem.* **1979**, *27*, 406–409.

Hansch, C.; Leo, A. *Substituent Constants for Correlation Analysis in Chemistry and Biology*; Wiley-Interscience: New York, 1979.

Hopfinger, A. J. *Conformational Properties of Macromolecules*; Academic Press: New York, 1973.

Hopfinger, A. J.; Burke, B. J. Molecular Shape Analysis: A Formalism to Quantitatively Establish Spatial Molecular Similarity. In *Concepts and Applications of Molecular Similarity*; Johnson, M. A., Maggiora, G. M., Eds.; Wiley: New York, 1990; Chapter 7, pp 173–209.

Hopfinger, A. J.; Pearlstein, R. A. Molecular Mechanics Force Field Parameterization Procedures. *J. Comput. Chem.* **1984**, *5*, 486–499.

Nicholas, J.; Martin, E.; Hopfinger, A. J. Conformational Analysis of Substituted Pyrazoline Ring Systems. *J. Phys. Chem.* **1994**, in press.

Pople, J. A.; Beveridge, D. A. *Approximate Molecular Orbital Theory*; McGraw-Hill: New York, 1970.

van Hes, R.; Wellinga, K.; Grosscurt, A. C. 1-Phenylcarbamoyl-2-pyrazolines: A New Class of Insecticides. 2. Synthesis and Insecticidal Properties of 3,5-Diphenyl-1-phenylcarbamoyl-2-pyrazolines. *J. Agric. Food Chem.* **1978**, *26*, 915–918.

Wellinga, K.; Grosscurt, A. C.; van Hes, R. 1-Phenylcarbamoyl-2-pyrazolines: A New Class of Insecticides. 1. Synthesis and Insecticidal Properties of 3-Phenyl-1-phenylcarbamoyl-2-pyrazolines. *J. Agric. Food Chem.* **1977**, *25*, 987–992.

Received for review July 12, 1993. Accepted November 23, 1993.[⊗]

[⊗] Abstract published in *Advance ACS Abstracts*, January 15, 1994.